CSMA 2026
17ème Colloque National en Calcul des Structures
18-22 Mai 2026, Presqu'île de Giens (Var)

Vibro-Acoustic Modeling of Aircraft Cabin Noise induced by Turbulent Boundary Layer Using Radiative Energy Transfer

T. Wanglomklang[1], F. Gillot[1], S. Besset[1], K. Shimoyama[2]

[1] *LTDS/D2S, École Centrale de Lyon, Ecully, France*
[2] *Department of Mechanical Engineering, Kyushu University, Fukuoka, Japan*

Résumé — This work presents a high-frequency vibro-acoustic modelling approach for predicting aircraft cabin noise induced by Turbulent Boundary Layer (TBL) excitation. The wall-pressure loading is represented using a semi-empirical spectrum combined with a spatial coherence reduction, enabling the construction of a physically consistent distributed surface source. The interior acoustic field is computed through a radiative energy transfer formulation in which each boundary element acts as an emitting–receiving patch, with energy exchanges governed by geometric visibility and local absorption. Numerical results obtained on a representative fuselage section show smooth and physically consistent energy distributions inside the cabin, reflecting the spatial variation of the aerodynamic excitation and the influence of the interior surfaces. The proposed method offers an efficient and physics-informed tool for early-stage cabin acoustic assessment and provides a basis for future optimisation developments.
Mots clés — High-frequency acoustics, Radiative Energy Transfer, Simplified Energy Method, Turbulent Boundary Layer, Aircraft Cabin Noise.

1 Introduction

During cruise conditions, aircraft cabin noise is dominated by the Turbulent Boundary Layer (TBL) acting on the external fuselage. At mid–high frequencies, the rapid increase in modal density makes deterministic FEM/BEM approaches computationally expensive. Energy-based formulations such as radiative energy transfer, and its discrete implementation through the energy method, provide a more suitable framework by transporting acoustic energy instead of phase-resolved pressure waves [6]. However, most applications of the energy method still rely on idealised internal point sources, which do not represent the spatially distributed and partially coherent nature of the wall-pressure field induced by the TBL. This broadband stochastic field is characterised by an auto-spectrum and spatial decay described by semi-empirical models such as Goody [4] and Corcos [3]. Experimental and modelling studies also report a strong non-uniformity in the transmission into the cabin, with lightweight structural regions generally radiating more acoustic energy than stiffened fuselage panels [7].

The present work extends the energy method by introducing a distributed TBL boundary source constructed directly from the wall-pressure spectrum and correlation lengths. This results in a physically consistent energy input on each surface patch and enables a more realistic prediction of the cabin acoustic field under TBL excitation.

2 Methodology

The proposed modelling chain predicts the interior acoustic field generated by the TBL loading applied over the external fuselage. The approach follows the radiative energy transfer method of Le Bot [6], implemented. The procedure consists of three steps : (i) modelling the external TBL wall-pressure field, (ii) mapping this excitation into an equivalent boundary energy flux, and (iii) solving for the interior acoustic transport using a energy integration equation.

2.1 Turbulent Boundary Layer Excitation

The turbulent boundary layer produces broadband wall-pressure fluctuations with finite spatial coherence. Recent aero-vibro-acoustic studies [8, 7, 5] show that this loading cannot be represented by a set of incoherent monopole sources. Instead, it must be treated as a distributed stochastic excitation characterised by correlation lengths in the streamwise and spanwise directions.

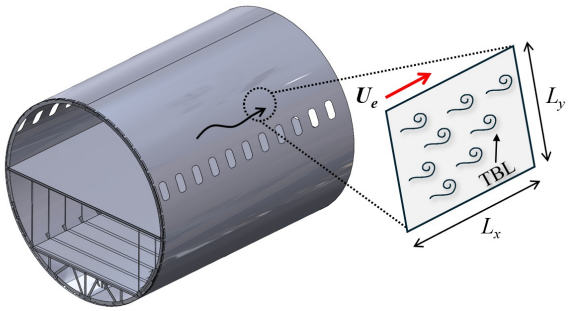

FIGURE 1 – Schematic of a panel excited by a Turbulent Boundary Layer (TBL).

Figure 1 illustrates the physical mechanism under consideration. The fluctuating pressure field convects in the streamwise direction with characteristic correlation lengths (L_x, L_y) that govern the spatial structure of the excitation.

2.1.1 Wall-Pressure Auto-Spectral Density

The frequency content of the wall-pressure field is obtained using the Goody model, which provides an empirical fit for zero-pressure-gradient boundary layers :

$$\phi_{pp}(\omega) = \frac{\tau_w^2 \delta}{U_e} \frac{C_2 \left(\frac{\omega\delta}{U_e}\right)^2}{\left[\left(\frac{\omega\delta}{U_e}\right)^{0.75} + C_1\right]^{3.7} + \left[C_3 \left(\frac{\omega\delta}{U_e}\right)\right]^7}, \tag{1}$$

where δ is the boundary-layer thickness, τ_w the wall shear stress, and U_e the boundary-layer edge velocity. The empirical constants are $C_1 = 0.5$, $C_2 = 3.0$, and $C_3 = 1.1 R_T^{-0.57}$ where R_T is a Reynolds number scaling parameter [4]. These aerodynamic quantities are extracted from cruise-flight conditions.

2.1.2 Spatial Correlation Model

The spatial correlation of pressure field between two points separated by (ξ_x, ξ_y) is described using the Corcos model :

$$S_n(\xi_x, \xi_y, \omega) = e^{-\left|\frac{\xi_x}{L_x}\right|} e^{-\left|\frac{\xi_y}{L_y}\right|} e^{-i\omega\frac{\xi_x}{U_c}} \tag{2}$$

where L_x and L_y denote the longitudinal and lateral correlation lengths, and U_c the convection speed. The complex phase term cannot be preserved in an energy-based solver. Only the real-valued coherence envelope is used to scale the effective radiating power of each surface patch.

2.1.3 Boundary Energy Flux

For a surface element P_j with area A_j, the turbulent boundary layer generates pressure fluctuations characterised by the wall-pressure auto-spectral density $\phi_{pp}(\omega)$. In an energy formulation, the mean-square pressure over a sufficiently small element may be approximated by the local spectrum,

$$\langle p^2(P_j, \omega) \rangle \simeq \phi_{pp}(\omega), \tag{3}$$

which gives the normally incident acoustic energy flux

$$q_{\mathrm{TBL}}(P_j,\omega) = \frac{\phi_{pp}(\omega)}{\rho_0 c}. \tag{4}$$

This expression maps the external wall-pressure loading directly into an equivalent acoustic flux, without explicitly resolving the structural vibrational response of the fuselage panels. The effect of the panel dynamics is instead absorbed into the local transmission coefficient $\tau_{TL}(P_j)$ introduced below, which accounts for the combined structural and acoustic filtering of the wall assembly.

The TBL pressure field is not coherent over arbitrarily large surfaces. Its streamwise and spanwise correlation scales, L_x and L_y, define a characteristic correlation area

$$A_{\mathrm{corr}} = L_x L_y. \tag{5}$$

When the discretised element area A_j greatly exceeds this correlation area, spatial averaging reduces the effective fluctuation level. Classical results for turbulent pressure fields [2, 1] indicate that the element-averaged mean-square pressure decreases approximately in proportion to A_{corr}/A_j :

$$\langle p^2\rangle_{\mathrm{elem}} \approx \langle p^2\rangle_{\mathrm{local}} \left(\frac{A_{\mathrm{corr}}}{A_j}\right), \qquad A_j \gg A_{\mathrm{corr}}. \tag{6}$$

Since an energy-based solver does not retain the detailed cross-spectral structure within each element, this effect is introduced through a coherence efficiency factor based on the ratio of the correlation area to the element area :

$$\eta_{\mathrm{coh}}(P_j) = \min\left(1, \frac{A_{\mathrm{corr}}}{A_j}\right), \tag{7}$$

which enforces full coherence for small elements and a physically consistent reduction for larger ones. This simplified formulation replaces the rigorous wavenumber-space integration of the cross-spectral density (i.e. the joint acceptance function) with an area-based scaling that captures the dominant effect of finite spatial coherence at moderate computational cost.

The energy injected into element P_j by the TBL is then written as

$$B_{\mathrm{TBL},j}(\omega) = q_{\mathrm{TBL}}(P_j,\omega) A_j \tau_{TL}(P_j) \eta_{\mathrm{coh}}(P_j), \tag{8}$$

where $\tau_{TL}(P_j)$ denotes the local transmission coefficient. This formulation delivers a surface-based excitation compatible with the radiative energy transfer framework while capturing the essential frequency- and correlation-dependent characteristics of a boundary layer.

2.2 Radiative Energy Transfer at Boundary

The emissive power $B(P,\omega)$ at each boundary element results from two mechanisms : (i)the energy injected through the external aerodynamic loading, and (ii) the energy received from other elements and re-emitted after partial absorption. Applying energy conservation leads to the boundary energy balance :

$$B(P,\omega) = (1-\alpha(P))\left[q_{\mathrm{TBL}}(P,\omega) + \int_\Gamma B(Q,\omega) F_{Q\to P}(\omega)\, dQ\right], \tag{9}$$

where $\alpha(P)$ is the absorption coefficient, $F_{Q\to P}$ is the view-factor kernel representing geometric energy transfer. Discretising Eq. (9) over N_b patches yields the linear system :

$$(\mathbf{I}-\mathbf{T})\mathbf{B} = \mathbf{B}_{\mathrm{TBL}}, \tag{10}$$

where $\mathbf{T}$ contains the view-factor interactions and $\mathbf{B}_{\mathrm{TBL}}$ is the vector of TBL-induced boundary energy injections.

2.3 Acoustic Energy Transmission

At high frequency, the acoustic wavelength becomes small compared with the cabin dimensions, preventing phase-resolved modelling. The interior field is therefore represented through an acoustic-energy integration equation :

$$W(M,\omega) = \int_{\Gamma} \frac{B(P,\omega)\cos\theta_{PM}}{4\pi c\,|PM|^2}\,dP, \tag{11}$$

where $B(P,\omega)$ is the unknown boundary emissive power, and θ_{PM} is the angle between the surface normal at P and the direction PM. Thus, solving the interior acoustic problem reduces to determining $B(P,\omega)$ on all cabin boundaries.

3 Numerical Application

This section demonstrates the implementation of the proposed modelling chain on a representative aircraft cabin segment. The objective is to assess the effect of the distributed TBL excitation on the interior acoustic field and to identify the dominant transmission paths. All numerical parameters given below correspond exactly to those used in the simulation.

3.1 Aircraft Cabin Model

The computational domain consists of a 10 m fuselage section with a circular cross-section truncated by the floor, as illustrated in Fig. 2. The interior cavity is discretised into 2958 planar boundary facets. Each facet is assigned an absorption coefficient and a transmission-loss value, and the same mesh is used consistently for the energy-transfer computation and for mapping the TBL excitation onto the interior surface. The coordinate system is defined such that the x-axis runs from nose to tail, the y-axis points starboard, and the z-axis is vertical. TBL excitation is applied only on the external fuselage (zones A, C and D in Fig. 2), while all other boundaries act purely as passive, absorbing and reflecting surfaces.

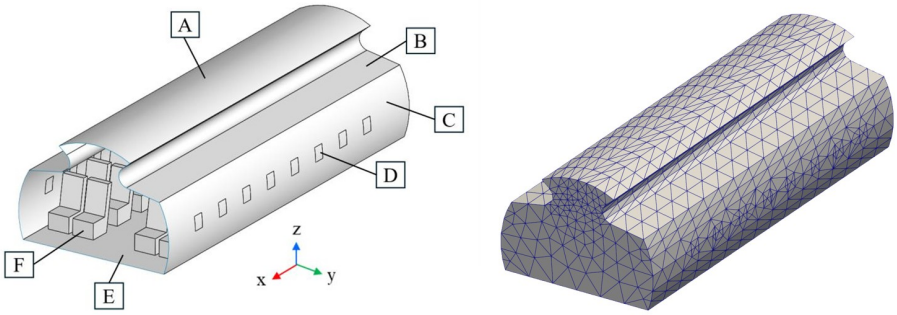

(a) Interior Cabin Model (b) Finite Element Model

FIGURE 2 – Cabin geometry used in the simulations. (a) Interior cavity ; (b) Surface discretisation with 2958 elements.

3.2 TBL Excitation Parameters

The distributed aerodynamic loading is generated using wall-pressure spectrum and spatial coherence, following the methodology outlined in Section 2. The numerical values used for the TBL excitation in the present cabin configuration are summarised in Table 2. These parameters define the wall-pressure spectrum, the spatial correlation scale, and the coherent input power transmitted through each boundary element. The transmission-loss values assigned to the fuselage and window regions are representative of typical stiffened fuselage panels and lightweight window assemblies. The lower TL of window structures is expected from classical panel radiation, where lightweight and more compliant surfaces radiate

TABLE 1 – Geometrical domain, absorption coefficients and transmission loss used in the simulations.

Description	**Value**
Discretised boundary elements	2958
Geometry bounds (x, y, z)	$(0.0, -10.0)$, $(-2.0, 2.0)$, $(-0.7, 2.0)$ m
Absorption coefficients	
α_{ceiling}, α_{luggage}, α_{walls}	0.20, 0.15, 0.15
α_{windows}, α_{floor}, α_{seats}	0.15, 0.60, 0.70
Transmission-loss at excitation surfaces	
Fuselage wall panels	45 dB
Upper fuselage belt	40 dB
Windows	22 dB

more efficiently than stiffened panels [1, 2]. These values are not intended to reproduce a specific aircraft design but to provide physically realistic contrasts for evaluating the distributed TBL excitation configuration.

TABLE 2 – TBL excitation parameters used for the distributed aerodynamic loading.

Parameter	**Value**
Flight speed U_e	$250\,\text{m/s}$
Convection speed U_c	$0.7U_e$
Corcos decay parameters (a_x, a_y)	$(0.116, 0.7)$
Analysis frequency f	1000 Hz
Speed of sound c	$343\,\text{m/s}$
Air density ρ_0	$1.21\,\text{kg/m}^3$
Boundary-layer thickness $\delta(x)$	0.01–0.15 m
Reference intensity I_{ref}	10^{-12} W/m^2

4 Results and Discussion

4.1 Surface energy distribution and interior SPL distribution

Figure 3 shows the two main outputs of the proposed high-frequency modelling chain : (a) the distributed TBL-induced boundary excitation mapped over the external fuselage belt, and (b) the resulting interior SPL distribution obtained from the radiative energy transfer.

The wall-pressure loading generated by the Goody model reproduces the expected longitudinal evolution of the turbulent boundary layer : higher excitation levels appear upstream where the boundary layer is thin, followed by a gradual decrease toward the downstream region. The spatial pattern develops smoothly on the triangulated fuselage surface, indicating that the proposed formulation is not sensitive to the underlying mesh discretisation. Although the external TBL loading is applied continuously over the fuselage belt, the effective transmitted energy into the cabin is strongly non-uniform. Owing to their significantly lower transmission loss compared with standard fuselage panels, the windows act as dominant airborne leakage paths. In Fig. 3(a), these regions appear as localised high-intensity patches, effectively behaving as secondary internal radiators. This behaviour is consistent with the expected effect of transmission-loss differences between structural regions, where the low-TL window belt naturally radiates more energy than the surrounding fuselage panels. The resulting interior SPL field (Fig. 3(b)) exhibits a smooth and physically consistent decay inside the cabin volume. The highest levels occur in the vicinity of the window region, then decrease gradually due to geometric spreading and the combined absorption of the seats, floor and ceiling. The SPL distribution does not show numerical artefacts or mesh-dependent irregularities, confirming that both the view-factor integration and the distributed-source

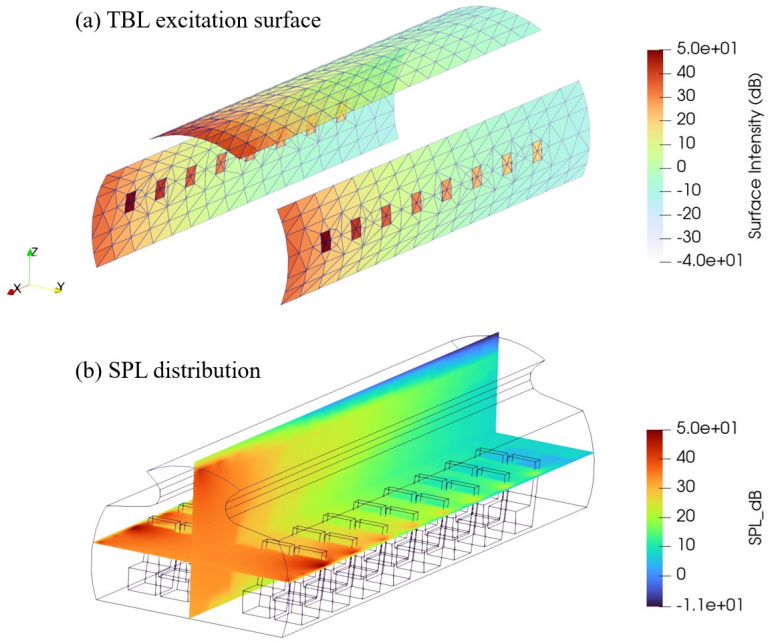

FIGURE 3 – (a) TBL-induced surface excitation applied on the external fuselage ; (b) Interior SPL distribution computed using the radiative energy transfer.

mapping operate robustly.

The present simulation focuses on a representative frequency and relies on simplified aerodynamic inputs, including a linearly growing boundary-layer thickness and a coherence scaling based solely on correlation area. Structural–acoustic coupling and local variations of transmission loss are not considered. Despite these simplifications, the method captures the dominant TBL-induced transmission mechanisms and provides a reliable foundation for future broadband and multi-parameter analyses.

4.2 Spectral analysis at interior receiver points

To further investigate the frequency dependence of the cabin noise, a spectral analysis was performed at two receiver locations positioned at ear height in the passenger seating area : Test Pos. 1 at (5.8, 0.8, 0.3) m and Test Pos. 2 at (3.8, 0.8, 0.3) m, as shown in Fig. 4(a). The resulting Sound Pressure Level (SPL) spectra, computed from 100 Hz to 5000 Hz, are presented in Fig. 4(b).

The predicted spectra exhibit the characteristic decay expected of TBL-induced interior noise. At low frequencies (approximately 100 Hz), the interior SPL reaches 65–68 dB due to the high-energy content of large turbulent eddies and their relatively large correlation scales compared with the panel dimensions. As frequency increases, the SPL decreases monotonically, driven by both the spectral roll-off of the wall-pressure model and the reduced radiation efficiency of the fuselage panels at shorter structural wavelengths. The trend is fully consistent with the spatial distribution shown earlier in Fig. 3(b), confirming the coherence between the boundary excitation model and the radiative energy transfer computation. Moreover, the close similarity between the two receiver spectra suggests that the cabin mid-section behaves as a relatively diffuse acoustic field, with only modest longitudinal variation despite the changes in boundary excitation along the fuselage.

5 Conclusion

A high-frequency energy-based method has been presented to predict cabin noise induced by Turbulent Boundary Layer (TBL) excitation. The approach constructs a distributed surface excitation and evaluates the interior acoustic field using a radiative energy transfer formulation. The results show smooth and physically consistent energy distributions inside the cabin, reflecting the spatial variation of the aerodynamic loading together with the effects of geometry and boundary absorption. The method provides

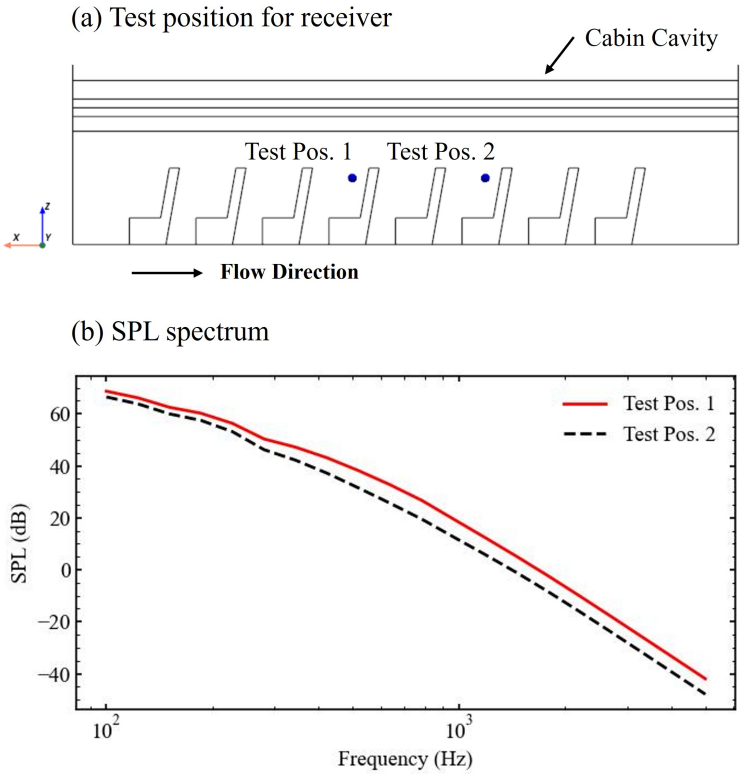

FIGURE 4 – (a) Location of the two interior receiver points (Test Pos. 1 and Test Pos. 2) within the cabin cavity ; (b) Computed Sound Pressure Level (SPL) spectra showing the frequency decay from 100 Hz to 5000 Hz at the two receiver locations.

an efficient tool for early-stage acoustic assessment without relying on phase-resolved simulations. In future work, the focus will be on improved transmission modelling, comparison between experimental values and our simulations, and integration into optimisation workflows for cabin noise reduction. Further detailed discussion of these aspects will be provided during the presentation.

Références

[1] W. K. Blake, *Mechanics of Flow-Induced Sound and Vibration*, Academic Press, 1986.

[2] D. M. Chase, *Modeling the Wavevector-Frequency Spectrum of Wall Pressure Under a Turbulent Boundary Layer*, Journal of Sound and Vibration, 70(1), 1976.

[3] G. M. Corcos, *Resolution of Pressure in Turbulence*, Journal of the Acoustical Society of America, 35(2), 1963.

[4] M. Goody, *Empirical Prediction of Turbulent Boundary Layer Wall Pressure Fluctuations*, AIAA Journal, 42(9), 2004.

[5] D. Juvé, M. Berton, E. Salze, *Spectral Properties of Wall-Pressure Fluctuations and Their Estimation from Computational Fluid Dynamics*, in : *Flinovia - Flow Induced Noise and Vibration Issues*, Springer, 27–46, 2015.

[6] A. Le Bot, *Comparison of an integral equation on energy and the ray-tracing technique in room acoustics*, Journal of the Acoustical Society of America, 108(4), 2000.

[7] R. Leneveu, M. Rissmann, A. Alonso, E. Salze, *Full-Scale Cabin Noise from Turbulent Boundary Layer Excitation, Part 2 : Vibroacoustic Modelling and Transmission*, Proceedings of ICSV26, Montreal, 2019.

[8] B. Plouseau-Guédé, L. Polacchini, A. Lebrun, E. Deck, A. Misdariis, *Similitude Laws for Scaling Vibrations and Acoustic Radiation of Panels Excited by a Turbulent Boundary Layer*, in : AIAA–CEAS Aeroacoustics Conference (Flinovia IV), Springer, 2025 (preprint).